

The crystal structures of Fe-bearing MgCO_3 sp^2 - and sp^3 -carbonates at 98 GPa from single-crystal X-ray diffraction using synchrotron radiation

Stella Chariton,^{a,f*} Maxim Bykov,^a Elena Bykova,^b Egor Koemets,^a Timofey Fedotenko,^c Björn Winkler,^d Michael Hanfland,^e Vitali B. Prakapenka,^f Eran Greenberg,^f Catherine McCammon^a and Leonid Dubrovinsky^a

Received 29 January 2020

Accepted 17 April 2020

Edited by M. Weil, Vienna University of Technology, Austria

Keywords: carbonates; magnesite-II; sp^3 -carbonates; sp^2 -carbonates; crystal structure; high-pressure single-crystal X-ray diffraction.

CCDC references: 1998018; 1998019

Supporting information: this article has supporting information at journals.iucr.org/e

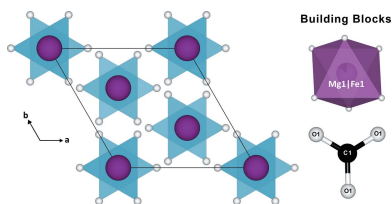
^aBayerisches Geoinstitut, University of Bayreuth, 95440 Bayreuth, Germany, ^bDeutsches Elektronen-Synchrotron (DESY), 22607 Hamburg, Germany, ^cMaterial Physics and Technology at Extreme Conditions, Laboratory of Crystallography, University of Bayreuth, 95440 Bayreuth, Germany, ^dInstitute of Geosciences, Goethe University, 60438 Frankfurt am Main, Germany, ^eEuropean Synchrotron Radiation Facility, BP 220, 38043 Grenoble Cedex, France, and ^fGeoSoilEnviroCARS, University of Chicago, 60637 Chicago, Illinois, USA. *Correspondence e-mail: stellachariton@hotmail.com

The crystal structure of MgCO_3 -II has long been discussed in the literature where DFT-based model calculations predict a pressure-induced transition of the carbon atom from the sp^2 to the sp^3 type of bonding. We have now determined the crystal structure of iron-bearing MgCO_3 -II based on single-crystal X-ray diffraction measurements using synchrotron radiation. We laser-heated a synthetic $(\text{Mg}_{0.85}\text{Fe}_{0.15})\text{CO}_3$ single crystal at 2500 K and 98 GPa and observed the formation of a monoclinic phase with composition $(\text{Mg}_{2.53}\text{Fe}_{0.47})\text{C}_3\text{O}_9$ in the space group $C2/m$ that contains tetrahedrally coordinated carbon, where CO_4^{4-} tetrahedra are linked by corner-sharing oxygen atoms to form three-membered $\text{C}_3\text{O}_9^{6-}$ ring anions. The crystal structure of $(\text{Mg}_{0.85}\text{Fe}_{0.15})\text{CO}_3$ (magnesium iron carbonate) at 98 GPa and 300 K is reported here as well. In comparison with previous structure-prediction calculations and powder X-ray diffraction data, our structural data provide reliable information from experiments regarding atomic positions, bond lengths, and bond angles.

1. Chemical context

Carbonates and their high-pressure behaviour have attracted significant interest because of their potential role as carbon-bearing phases in the deep Earth. Recent discoveries of novel compounds that contain tetrahedral CO_4^{4-} units (e.g., Merlini *et al.*, 2015; Cerantola *et al.*, 2017) increase the relevance of such studies, as the new high-pressure phases may be stable at conditions prevalent in the deep part of Earth's lower mantle. In addition, theoretical modelling predictions imply potential structural analogues of CO_4^{4-} -bearing carbonates and silicates, and thus carbonates with tetrahedrally coordinated carbon may be important to understanding the complex geochemistry of Earth's mantle.

Carbonates with tetrahedrally coordinated carbon are not well characterized, despite their potential significance, as structural studies have to be carried out under high-pressure conditions and are therefore challenging. A reliable structural characterization is, however, a prerequisite for determining phase stabilities and to understand, for example, why the p , T -phase diagram of MgCO_3 is relatively simple compared to the dense phase diagram of CaCO_3 (see summary in Bayarjargal *et al.*, 2018).



It is generally accepted that magnesite (MgCO_3) transforms to $\text{MgCO}_3\text{-II}$ at 80–115 GPa (Isshiki *et al.*, 2004; Boulard *et al.*, 2011, 2015; Maeda *et al.*, 2017). Models based on density functional theory (DFT) (Oganov *et al.*, 2008) and interpretation of X-ray diffraction data and IR spectra imply that $\text{MgCO}_3\text{-II}$ contains carbon in a tetrahedral coordination (Boulard *et al.* 2011, 2015). While structure-prediction techniques are undoubtedly useful for preliminary surveys of phase stabilities, they provide a range of possible new phases, derived under constraints such as unit-cell contents. Powder diffraction data obtained at pressures around 100 GPa generally do not yield accurate structure determinations, and typically do not allow unambiguous assignment of the space group or site occupancies. In contrast, single-crystal X-ray diffraction is a powerful and unique tool that can provide accurate structure refinements under these conditions (Boffa Ballaran *et al.*, 2013). Well-established statistical parameters allow an assessment of the reliability of the structural model. Other carbonate structures with tetrahedral CO_4^{4-} units at extreme conditions have previously been reported using this method, such as the novel phases $\text{Fe}_4\text{C}_3\text{O}_{12}$ in space group $R\bar{3}c$, $(\text{Mg,Fe})_4\text{C}_4\text{O}_{13}$ in $C2/c$ (Merlini *et al.*, 2015; Cerantola *et al.*, 2017) and $\text{Ca}(\text{Fe,Mg})_2\text{C}_3\text{O}_9$ in $Pnma$ (Merlini *et al.*, 2017). These results lead to two conclusions. Firstly, the stability fields of carbonates strongly depend on their composition. Secondly, CO_4^{4-} units have the ability to form polymeric networks, and thus are potential analogues to silicates.

2. Structural commentary

Under ambient conditions $(\text{Mg}_{0.85}\text{Fe}_{0.15})\text{CO}_3$ crystallizes in the calcite-type structure in space group $R\bar{3}c$. Iron and magnesium share the same crystallographic site (Wyckoff position $6b$; site symmetry $\bar{3}$.) and are coordinated by six oxygen atoms, while the CO_3^{2-} units form planar equilateral triangles with point-group symmetry 32 (e.g. Lavina *et al.*, 2010). After compression to 98 (2) GPa at ambient temperature, X-ray diffraction data of $(\text{Mg}_{0.85}\text{Fe}_{0.15})\text{CO}_3$ can still be indexed in the $R\bar{3}c$ space group (Fig. 1, Table 1). However, the unit-cell volume is decreased by nearly 32% compared to ambient conditions.

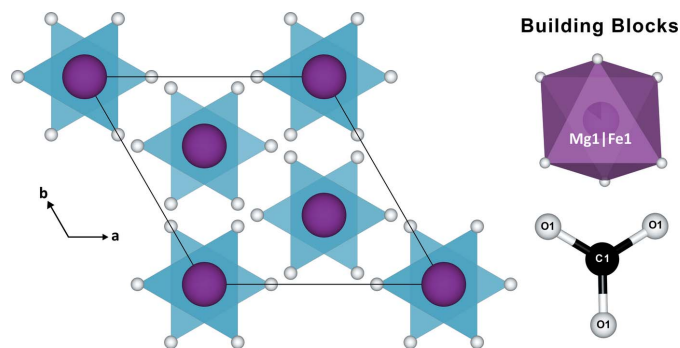


Figure 1

Crystal structure of $(\text{Mg}_{0.85}\text{Fe}_{0.15})\text{CO}_3$ at 98 GPa and prior to laser-heating shown in a projection along the c axis. The building blocks of the unit cell appear on the right. Here, iron occupies the same sites as the magnesium atoms.

This result challenges a recent suggestion based on DFT-based calculations that predicted a structural transformation of MgCO_3 to a triclinic phase at 85–101 GPa and 300 K (Pickard & Needs, 2015). At 98 GPa, the C–O bond length [1.195 (8) Å] has decreased only by $\sim 7\%$ compared to the structure at ambient conditions, thus reflecting the highly incompressible nature of the CO_3^{2-} units. On the other hand, the (Mg/Fe)–O bonds [1.855 (5) Å at 98 GPa] display a much more compressible behavior ($\sim 12\%$ bond-length and $\sim 32\%$ octahedra-volume shrinkage compared to ambient conditions). On a last note, it is well known that rhombohedral carbonates can be described as a distortion of the NaCl (B1) structure. Previously, the t parameter, $t = 4a/\sqrt{2}c$, where a and c are the lattice parameters) has been used to evaluate the degree of distortion (Gao *et al.*, 2014). We observed that at 98 GPa and 300 K, $t \simeq 1$ for $(\text{Mg}_{0.85}\text{Fe}_{0.15})\text{CO}_3$, which means that at the conditions of our experiment the (Mg/Fe) cations and the CO_3^{2-} anions are arranged in the manner of a nearly ideal NaCl (B1) structure.

After annealing at 2500 K and 98 GPa, we observed a phase transition to a polymorph in which carbon is tetrahedrally coordinated by oxygen. The newly formed phase with chemical formula $(\text{Mg}_{2.53}\text{Fe}_{0.47})\text{C}_3\text{O}_9$ (as determined from structural refinements, see below) has monoclinic symmetry, and the diffraction pattern indicates space group $C2/m$ (Fig. 2, Table 1). We identify this phase as the $\text{MgCO}_3\text{-II}$ structure that was previously predicted (Oganov *et al.*, 2008; Boulard *et al.*, 2015). In contrast to previous studies, we provide an accurate structure solution and refinement based on single crystal X-ray diffraction data. The structure consists of three-membered $\text{C}_3\text{O}_9^{6-}$ rings formed by corner-sharing CO_4 tetrahedra (Fig. 2c) that alternate with $[\text{Fe,Mg}]O_x$ polyhedra ($x = 6\text{--}8$) perpendicular to the b axis. We can distinguish three crystallographic cation positions (Fig. 2b):

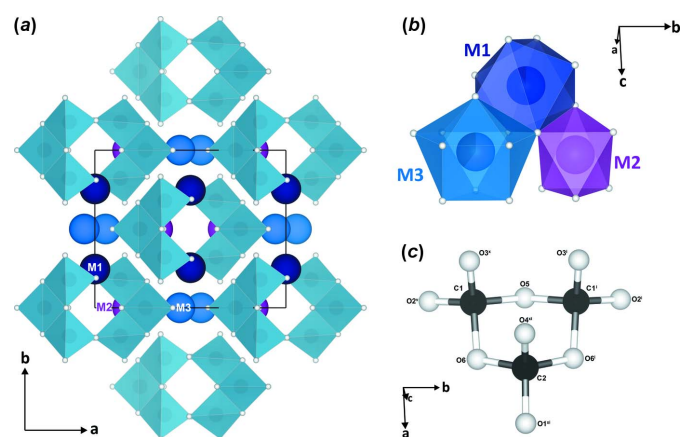


Figure 2

(a) The crystal structure of $(\text{Mg}_{2.53}\text{Fe}_{0.47})\text{C}_3\text{O}_9$ according to this study, in a projection along the c axis; CO_4 tetrahedra are given in the polyhedral representation. (b) The three cation sites that host Mg/Fe atoms and their respective polyhedra. (c) $\text{C}_3\text{O}_9^{6-}$ ring anions are formed from three edge-sharing CO_4 tetrahedra. Atomic positions are shaded according to colours in (b) and oxygen atoms appear as small white spheres. [Symmetry codes: (i) $x, -y, z$; (v) $-x + \frac{1}{2}, -y + \frac{1}{2}, -z + 1$; (x) $-x, y, -z + 1$; (xi) $x, y, z + 1$.]

Table 1
Experimental details.

	MgCO ₃ -II at 98 GPa	MgCO ₃ at 98 GPa
Crystal data		
Chemical formula	3[(Mg _{0.85} Fe _{0.15})CO ₃]	(Mg _{0.85} Fe _{0.15})CO ₃
<i>M_r</i>	265.6	89
Crystal system, space group	Monoclinic, <i>C2/m</i>	Trigonal, <i>R</i> $\bar{3}c$
Temperature (K)	293	293
<i>a</i> , <i>b</i> , <i>c</i> (Å)	8.238 (3), 6.5774 (12), 6.974 (5)	4.281 (7), 4.281 (7), 12.12 (2)
α , β , γ (°)	90, 104.40 (6), 90	90, 90, 120
<i>V</i> (Å ³)	366.0 (3)	192.3 (5)
<i>Z</i>	4	6
Radiation type	Synchrotron, $\lambda = 0.411107$ Å	Synchrotron, $\lambda = 0.2952$ Å
μ (mm ⁻¹)	0.58	0.25
Crystal size (mm)	0.01 × 0.01 × 0.01	0.01 × 0.01 × 0.01
Data collection		
Diffractometer	ID15b @ ESRF	13IDD @ APS (GSECARS)
Absorption correction	Multi-scan (<i>CrysAlis PRO</i> ; Rigaku OD, 2019)	Multi-scan (<i>CrysAlis PRO</i> ; Rigaku OD, 2019)
<i>T</i> _{min} , <i>T</i> _{max}	0.104, 1	0.95, 1
No. of measured, independent and observed [<i>I</i> > 3 σ (<i>I</i>)] reflections	522, 298, 211	176, 60, 33
<i>R</i> _{int}	0.020	0.053
(<i>sin</i> θ / λ) _{max} (Å ⁻¹)	0.860	0.900
Refinement		
<i>R</i> [<i>F</i> ² > 2 σ (<i>F</i> ²)], <i>wR</i> (<i>F</i> ²), <i>S</i>	0.084, 0.095, 3.21	0.100, 0.084, 2.89
No. of reflections	298	60
No. of parameters	39	5
$\Delta\rho_{\max}$, $\Delta\rho_{\min}$ (e Å ⁻³)	1.76, -1.21	0.66, -0.50

Computer programs: *CrysAlis PRO* (Rigaku OD, 2019), *SUPERFLIP* (Palatinus & Chapuis, 2007), *JANA2006* (Petříček *et al.*, 2014), *VESTA* (Momma & Izumi, 2011) and *publCIF* (Westrip, 2010).

(1) The *M1* site is located on a twofold rotation axis (Wyckoff position 4*g*) and is occupied by Mg and Fe in a 0.917 (17):0.083 (17) ratio. This site is surrounded by eight oxygen atoms forming a distorted square antiprism (dark blue); (2) The *M3* site is situated on a mirror plane (4 *i*) in a 0.61 (2):0.39 (2) Mg:Fe ratio and a coordination number of 10 (blue; can be described as half cuboctahedra merged through hexagonal-based faces with hexagonal pyramids); (3) *M2* is likewise situated on a mirror plane (4 *i*) and is fully occupied by Mg in [MgO₆] octahedra (magenta). The maximum and minimum bond lengths of each cation site from its neighbouring oxygen atoms are shown in Table 2. At 98 GPa the C—O bond lengths of the two different CO₄⁴⁻ carbonate groups [C1 is located on a general site (8 *j*) and C2 on a mirror plane (4 *i*) vary from 1.287 (18)–1.409 (13) Å and the C—O—C inter-tetrahedral angle is ~112°.

From all proposed structural models for MgCO₃-II over the last two decades, only one appears to successfully match the

structure model that we report here. On the basis of powder X-ray diffraction (PXRD) experiments and variable-cell simulations, Oganov *et al.* (2008) suggested several energetically favourable structural models for MgCO₃-II, one of which is in space group *C2/m*. While our structural solution and refinement from the experimental data is clearly similar to the theoretical predictions by Oganov *et al.* (2008), the different composition of the materials and the small differences in the structural parameters required us to check additionally whether theoretical calculations with our model as the starting one would lead to the same result as that reported by Oganov *et al.* (2008). We performed such a test and confirm that our results and those of Oganov *et al.* (2008) are the same within the accuracy of the methods. More concretely, we performed DFT-based model calculations using the plane wave/pseudopotential *CASTEP* package (Clark *et al.*, 2005). Pseudopotentials were generated ‘on the fly’ using the parameters provided with the *CASTEP* distribution. These pseu-

Table 2
Geometric parameters of (Mg_{2.53}Fe_{0.47})C₃O₉ at 98 GPa.

Group	Maximal bond length (Å)	Minimal bond length (Å)	Polyhedron volume (Å ³)	Distortion index ^a
CO ₄ (C1—O)	1.409 (19)	1.287 (18)	1.25	0.045
CO ₄ (C2—O)	1.38 (3)	1.29 (4)	1.25	0.022
M2O ₆ ^b	1.87 (3)	1.813 (10)	7.78	0.010
M1O ₈ ^c	2.039 (13)	1.908 (14)	13.24	0.020
M3O ₈ ^d	2.358 (14) ^e	1.828 (19)	14.59	0.068

Notes: (a) as defined in Baur (1974); (b) Mg:Fe ratio for *M* = 1:0; (c) Mg:Fe ratio for *M* = 0.917 (17):0.083 (17); (d) Mg:Fe ratio for *M* = 0.61 (2):0.39 (2); (e) alternatively, for CN = 10 the maximal distance is 2.451 (14) Å, the polyhedral volume is 20.58 Å³ and the distortion index is 0.080.

dopotentials have been tested extensively for accuracy and transferability (Lejaeghere *et al.*, 2016). The pseudopotentials were employed in conjunction with plane waves up to a kinetic energy cutoff of 1020 eV. The calculations were carried out with the PBE exchange–correlation function (Perdew *et al.*, 1996). For simplicity, we assumed that all three *M1*, *M2* and *M3* positions are fully occupied by Mg^{2+} . The calculations revealed that the energies of our structural model and that of Oganov *et al.* (2008) are indeed, identical. The DFT calculations gave C–O distances in good agreement with experimental data. Each carbon atom is coordinated by two oxygen atoms that are each shared with another tetrahedrally coordinated carbon, and two that are not shared. The C–O distances for the latter are significantly shorter [$1.29 \text{ \AA} < d(\text{C–O}) < 1.32 \text{ \AA}$] than the former [$1.33 \text{ \AA} < (\text{C–O}) < 1.41 \text{ \AA}$]. A Mulliken bond-population analysis shows that for the long C–O bonds there is a significant bond population of $\sim 0.5 \text{ e}^- \text{ \AA}^{-3}$. This is less than the value for the short bonds, where the bond population is $\sim 0.9 \text{ e}^- \text{ \AA}^{-3}$, but this still is a predominantly covalent bond, and justifies the description as a tetrahedrally coordinated carbon atom. The formation of $(\text{C}_3\text{O}_9)^{6-}$ carbonate rings was previously observed in

$\text{Ca}(\text{Fe},\text{Mg})\text{C}_3\text{O}_9$ (dolomite-IV) after laser heating of $\text{Ca}(\text{Fe},\text{Mg})\text{CO}_3$ at 115 GPa (Merlini *et al.*, 2017). However, dolomite-IV is topologically different from the MgCO_3 -II structure that we report here. Unlike $(\text{Mg}_{2.53}\text{Fe}_{0.47})\text{C}_3\text{O}_9$, $\text{Ca}(\text{Fe},\text{Mg})\text{C}_3\text{O}_9$ crystallizes in the orthorhombic system (space group *Pnma*), thus highlighting the significance of the metal cations that are present in the carbonate.

Upon decompression at ambient temperature, $(\text{Mg}_{2.53}\text{Fe}_{0.47})\text{C}_3\text{O}_9$ reflections become broad and weak, and almost disappear at ~ 74 GPa (Fig. 3*a–c*). This may be an indication of either amorphization or sluggish back-transformation to a carbonate with trigonal symmetry. Anticipating that further heating would aid recrystallization, we laser-heated the sample at 74 GPa and 2000 (150) K for a few seconds. Wide images collected on the temperature-quenched sample indicated the formation of the calcite structure-type carbonate (Fig. 3*d*).

3. Synthesis and crystallization

Magnesium carbonate crystals with $15(\pm 4)$ mol% Fe were grown following the procedure reported by Chariton *et al.* (2020). The composition of the starting material was determined by single-crystal X-ray diffraction under ambient conditions as $(\text{Mg}_{0.85}\text{Fe}_{0.15})\text{CO}_3$. A single crystal of $\sim 7 \mu\text{m}$ size in all dimensions was loaded inside the sample chamber of a BX90-type diamond anvil cell equipped with bevelled Bohler–Almax type diamonds (culet diameter 80 mm). Rhenium and neon were used as the gasket material and pressure-transmitting medium, respectively. The pressure was determined using the equation of state (EoS) of solid Ne (Fei *et al.*, 2007). First, the sample was compressed up to 98 GPa and a single-crystal collection took place at 300 K. Consequently, the same crystal was laser-heated from both sides up to 2500 (150) K for a few seconds and then quenched to room temperature. Finally, we performed a 5×5 grid of still-image collection with a $2 \mu\text{m}$ step and 1 s exposure time around the center of the sample. This strategy was used to locate the most heated area of the crystal and the best spot to collect single-crystal X-ray diffraction patterns during rotation of the cell. Single-crystal data collection was performed as a series of ω scans over the range $\pm 35^\circ$ with a step of 0.5° .

4. Refinement

Details of the data collection, structure solution and refinement are summarized in Table 1. In the case of the $(\text{Mg}_{0.85}\text{Fe}_{0.15})\text{CO}_3$ dataset collected at 98 GPa, the limited number of available reflections required us to fix the Fe content according to our ambient condition estimates (see also "Synthesis and Crystallization" section). On the other hand, during the structure refinements of $(\text{Mg}_{2.53}\text{Fe}_{0.47})\text{C}_3\text{O}_9$ all three cation sites (i.e. *M1*, *M2* and *M3*) were tested for their ability to host Fe by refining the site occupancies. As described above, only the *M1* and *M3* sites were eventually found to accommodate $\sim 16(\pm 3)$ mol % Fe in total. Note that the resulting 5.38 Mg:Fe ratio of $(\text{Mg}_{2.53}\text{Fe}_{0.47})\text{C}_3\text{O}_9$ is almost

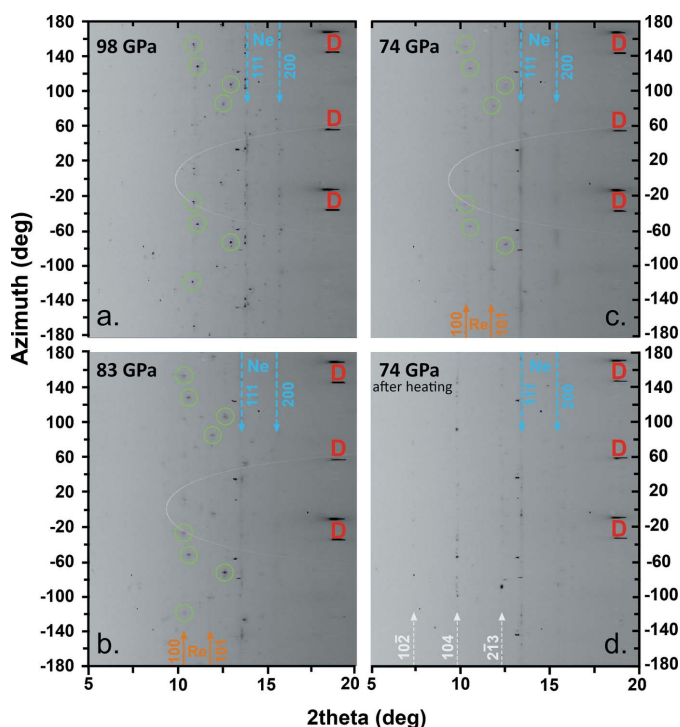


Figure 3 Unrolled X-ray diffraction images collected at room temperature ($\lambda = 0.411 \text{ \AA}$). (a) Sharp and intense reflections of $(\text{Mg}_{2.53}\text{Fe}_{0.47})\text{C}_3\text{O}_9$ appear after laser-heating of the starting material at 98 GPa and 2500 K. (b) The crystal phase gradually deteriorates during decompression and (c) nearly disappears at ~ 74 GPa. (d) Consequent laser-heating treatment results in the formation of the initial carbonate structure. Green circles mark a few of the characteristic reflections of $(\text{Mg}_{2.53}\text{Fe}_{0.47})\text{C}_3\text{O}_9$, the position of Ne reflections and in some cases Re reflections are marked with blue and orange arrows, respectively. The 2θ positions of three characteristic carbonate ($R\bar{3}c$) reflections are indicated with white arrows. Diamond reflections are marked in red.

identical to the starting 5.67 Mg:Fe ratio of $(\text{Mg}_{0.85}\text{Fe}_{0.15})\text{CO}_3$ within the accuracy of our method. Therefore, it is safe to conclude that nearly none or only a negligible amount of Fe was lost during the observed phase transition. The crystal structure of $(\text{Mg}_{2.53}\text{Fe}_{0.47})\text{C}_3\text{O}_9$ solved at 98 GPa was used for the structure refinements of the data of the same phase collected during decompression. Due to the limited angular range caused by the laser-heated DAC, the resolution of the data set was not sufficient to refine the anisotropic displacement parameters. Therefore, all atoms were refined with the isotropic approximation.

Acknowledgements

The large majority of diffraction experiments were performed on the X-ray diffraction beamline ID15b at the European Synchrotron Radiation Facility, Grenoble, France. Portions of this work were performed at GeoSoilEnviroCARS (The University of Chicago, Sector 13), Advanced Photon Source, Argonne National Laboratory.

Funding information

GeoSoilEnviroCARS is supported by the National Science Foundation – Earth Sciences (EAR – 1634415) and Department of Energy – GeoSciences (DE-FG02–94ER14466). This research used resources of the Advanced Photon Source, a US Department of Energy (DOE) Office of Science User Facility operated for the DOE Office of Science by Argonne National Laboratory under Contract No. DE-AC02–06CH11357. The project was supported by funds from the German Science Foundation (DFG) through the CarboPaT Research Unit FOR2125 (Mc3/20, Du393/9, Wi 1232) and the German Federal Ministry for Education and Research (BMBF).

References

- Baur, W. H. (1974). *Acta Cryst.* **B30**, 1195–1215.
- Bayarjargal, L., Fruhner, C.-J., Schrodt, N. & Winkler, B. (2018). *PEPI*, **281**, 31–45.
- Boffa Ballaran, T., Kurnosov, A. & Trots, D. (2013). *High. Press. Res.* **33**, 453–465.
- Boulard, E., Gloter, A., Corgne, A., Antonangeli, D., Auzende, A.-L., Perrillat, J.-P., Guyot, F. & Fiquet, G. (2011). *PNAS*, **108**, 5184–5187.
- Boulard, E., Pan, D., Galli, G., Liu, Z. & Mao, W. (2015). *Nat. Commun.* **6**, 6311.
- Cerantola, V., Bykova, E., Kuppenko, I., Merlini, M., Ismailova, L., McCammon, C., Bykov, M., Chumakov, A. I., Petitgirard, S., Kantor, I., Svitlyk, V., Jacobs, J., Hanfland, M., Mezouar, M., Prescher, C., Rüffer, R., Prakapenka, V. B. & Dubrovinsky, L. (2017). *Nat. Commun.* **8**, 15960.
- Chariton, S., McCammon, C., Vasiukov, D. M., Stekiel, M., Kantor, A., Cerantola, V., Kuppenko, I., Fedotenko, T., Koemets, E., Hanfland, M., Chumakov, A. I. & Dubrovinsky, L. (2020). *Am. Mineral.* **105**, 325–332.
- Clark, S. J., Segall, M. D., Pickard, C. J., Hasnip, P. J., Probert, M. J., Refson, K. & Payne, M. C. (2005). *Z. Kristallogr.* **220**, 567–570.
- Fei, Y., Ricolleau, A., Frank, M., Mibe, K., Shen, G. & Prakapenka, V. B. (2007). *PNAS*, **104**, 9182–9186.
- Gao, J., Zhu, F., Lai, X.-J., Huang, R., Qin, S., Chen, D.-L., Liu, J., Zheng, L.-R. & Wu, X. (2014). *High. Press. Res.* **34**, 89–99.
- Isshiki, M., Irifune, T., Hirose, K., Ono, S., Ohishi, Y., Watanuki, T., Nishibori, E., Takata, M. & Sakata, M. (2004). *Nature*, **427**, 60–63.
- Lavina, B., Dera, P., Downs, R. T., Tschauer, O., Yang, W., Shebanova, O. & Shen, G. (2010). *High. Press. Res.* **30**, 224–229.
- Lejaeghere, K., Bihlmayer, G., Björkman, T., Blaha, P., Blügel, S., Blum, V., Caliste, D., Castellì, I. E., Clark, S., Dal Corso, A., de Gironcoli, S., Deutsch, T., Dewhurst, J. K., Di Marco, I., Draxl, C., Dulak, M., Eriksson, O., Flores-Livas, J. A., Garrity, K. F., Genovese, L., Giannozzi, P., Giantomassi, M., Goedecker, S., Gonze, X., Grånäs, O., Gross, E. K., Gulans, A., Gygi, F., Hamann, D. R., Hasnip, P. J., Holzwarth, N. A., Iușan, D., Jochym, D. B., Jollet, F., Jones, D., Kresse, G., Koepf, K., Küçükbenli, E., Kvashnin, Y. O., Loch, I. L., Lubeck, S., Marsman, M., Marzari, N., Nitzsche, U., Nordström, L., Ozaki, T., Paulatto, L., Pickard, C. J., Poelmans, W., Probert, M. I., Refson, K., Richter, M., Rignanese, G. M., Saha, S., Scheffler, M., Schlipf, M., Schwarz, K., Sharma, S., Tavazza, F., Thunström, P., Tkatchenko, A., Torrent, M., Vanderbilt, D., van Setten, M. J., Van Speybroeck, V., Wills, J. M., Yates, J. R., Zhang, G. X. & Cottenier, S. (2016). *Science*, pp. 351 aad3000.
- Maeda, F., Ohtani, E., Kamada, S., Sakamaki, T., Hirao, N. & Ohishi, Y. (2017). *Sci. Rep.* **7**, 40602.
- Merlini, M., Cerantola, V., Gatta, G. D., Gemmi, M., Hanfland, M., Kuppenko, I., Lotti, P., Müller, H. & Zhang, L. (2017). *Am. Mineral.* **102**, 1763–1766.
- Merlini, M., Hanfland, M., Salamat, A., Petitgirard, S. & Müller, H. (2015). *Am. Mineral.* **100**, 2001–2004.
- Momma, K. & Izumi, F. (2011). *J. Appl. Cryst.* **44**, 1272–1276.
- Oganov, A. R., Ono, S., Ma, Y., Glass, C. W. & Garcia, A. (2008). *Earth Planet. Sci. Lett.* **273**, 38–47.
- Palatinus, L. & Chapuis, G. (2007). *J. Appl. Cryst.* **40**, 786–790.
- Perdew, J. P., Burke, K. & Ernzerhof, M. (1996). *Phys. Rev. Lett.* **77**, 3865–3868.
- Petříček, V., Dušek, M. & Palatinus, L. (2014). *Z. Kristallogr.* **229**, 345–352.
- Pickard, C. J. & Needs, R. J. (2015). *Phys. Rev. B*, **91**, 104101.
- Rigaku OD (2019). *CrysAlis PRO*. Rigaku Oxford Diffraction Ltd, Yarnton, England.
- Westrip, S. P. (2010). *J. Appl. Cryst.* **43**, 920–925.

supporting information

Acta Cryst. (2020). E76, 715-719 [https://doi.org/10.1107/S2056989020005411]

The crystal structures of Fe-bearing MgCO₃ *sp*²- and *sp*³-carbonates at 98 GPa from single-crystal X-ray diffraction using synchrotron radiation

Stella Chariton, Maxim Bykov, Elena Bykova, Egor Koemets, Timofey Fedotenko, Björn Winkler, Michael Hanfland, Vitali B. Prakapenka, Eran Greenberg, Catherine McCammon and Leonid Dubrovinsky

Computing details

For both structures, data collection: *CrysAlis PRO* (Rigaku OD, 2019); cell refinement: *CrysAlis PRO* (Rigaku OD, 2019); data reduction: *CrysAlis PRO* (Rigaku OD, 2019); program(s) used to solve structure: Superflip (Palatinus & Chapuis, 2007); program(s) used to refine structure: Jana2006 (Petříček *et al.*, 2014); molecular graphics: *VESTA* (Momma & Izumi, 2011); software used to prepare material for publication: *publCIF* (Westrip, 2010).

Magnesium(II) iron(II) carbonate (MgCO₃-II_98GPa)

Crystal data

3[(Mg_{0.85}Fe_{0.15})CO₃]
 $M_r = 265.6$
 Monoclinic, *C2/m*
 Hall symbol: -C 2y
 $a = 8.238$ (3) Å
 $b = 6.5774$ (12) Å
 $c = 6.974$ (5) Å
 $\beta = 104.40$ (6)°
 $V = 366.0$ (3) Å³
 $Z = 4$

$F(000) = 530$
 $D_x = 4.861$ Mg m⁻³
 Synchrotron radiation, $\lambda = 0.41107$ Å
 Cell parameters from 146 reflections
 $\theta = 2.3$ – 19.0 °
 $\mu = 0.58$ mm⁻¹
 $T = 293$ K
 Irregular, colourless
 $0.01 \times 0.01 \times 0.01$ mm

Data collection

ID15b @ ESRF
 diffractometer
 Radiation source: synchrotron
 Synchrotron monochromator
 ω scans
 Absorption correction: multi-scan
 (CrysAlisPro; Rigaku OD, 2019)
 $T_{\min} = 0.104$, $T_{\max} = 1$

522 measured reflections
 298 independent reflections
 211 reflections with $I > 3\sigma(I)$
 $R_{\text{int}} = 0.020$
 $\theta_{\max} = 20.7$ °, $\theta_{\min} = 2.3$ °
 $h = -11 \rightarrow 12$
 $k = -8 \rightarrow 8$
 $l = -7 \rightarrow 9$

Refinement

Refinement on F
 Least-squares matrix: full
 $R[F^2 > 2\sigma(F^2)] = 0.084$
 $wR(F^2) = 0.095$
 $S = 3.21$

298 reflections
 39 parameters
 0 restraints
 5 constraints

Weighting scheme based on measured s.u.'s $w = 1/(\sigma^2(F) + 0.000144F^2)$
 $(\Delta/\sigma)_{\max} = 0.001$

$\Delta\rho_{\max} = 1.76 \text{ e } \text{\AA}^{-3}$
 $\Delta\rho_{\min} = -1.21 \text{ e } \text{\AA}^{-3}$

Fractional atomic coordinates and isotropic or equivalent isotropic displacement parameters (\AA^2)

	<i>x</i>	<i>y</i>	<i>z</i>	$U_{\text{iso}}^*/U_{\text{eq}}$	Occ. (<1)
Mg3	0.4441 (6)	0	0.6503 (9)	0.0177 (11)*	0.61 (2)
Fe3	0.4441 (6)	0	0.6503 (9)	0.0177 (11)*	0.39 (2)
Mg2	0.1712 (7)	0	0.3146 (12)	0.0086 (11)*	
Mg1	0	0.2457 (6)	0	0.0117 (13)*	0.917 (17)
Fe1	0	0.2457 (6)	0	0.0117 (13)*	0.083 (17)
O4	0.1395 (17)	0	0.044 (3)	0.020 (2)*	
O6	0.2736 (13)	0.1662 (9)	0.847 (2)	0.0179 (17)*	
O2	0.3442 (12)	0.1683 (9)	0.4218 (18)	0.0157 (15)*	
O1	0.4097 (18)	0	0.105 (3)	0.021 (2)*	
O5	0.1487 (16)	0	0.575 (3)	0.016 (2)*	
O3	0.0062 (12)	0.1898 (9)	0.2702 (19)	0.0159 (17)*	
C1	0.1347 (19)	0.1774 (13)	0.683 (3)	0.017 (2)*	
C2	0.265 (3)	0	0.964 (4)	0.024 (3)*	

Geometric parameters (\AA , $^\circ$)

Mg3—O6	2.451 (14)	Mg2—O3 ⁱ	1.814 (9)
Mg3—O6 ⁱ	2.451 (14)	Mg1—O4	1.962 (8)
Mg3—O2	1.947 (11)	Mg1—O4 ^{vi}	1.962 (8)
Mg3—O2 ⁱⁱ	2.226 (11)	Mg1—O6 ^v	1.991 (10)
Mg3—O2 ⁱⁱⁱ	2.226 (11)	Mg1—O6 ^{vii}	1.991 (10)
Mg3—O2 ⁱ	1.947 (11)	Mg1—O1 ^{viii}	2.039 (12)
Mg3—O1 ⁱⁱ	1.829 (18)	Mg1—O1 ^{ix}	2.039 (12)
Mg3—O5	2.359 (14)	Mg1—O3	1.908 (13)
Mg3—O3 ^{iv}	2.127 (7)	Mg1—O3 ^{vi}	1.908 (13)
Mg3—O3 ^v	2.127 (7)	Fe1—O4	1.962 (8)
Fe3—O6	2.451 (14)	Fe1—O4 ^{vi}	1.962 (8)
Fe3—O6 ⁱ	2.451 (14)	Fe1—O6 ^v	1.991 (10)
Fe3—O2	1.947 (11)	Fe1—O6 ^{vii}	1.991 (10)
Fe3—O2 ⁱⁱ	2.226 (11)	Fe1—O1 ^{viii}	2.039 (12)
Fe3—O2 ⁱⁱⁱ	2.226 (11)	Fe1—O1 ^{ix}	2.039 (12)
Fe3—O2 ⁱ	1.947 (11)	Fe1—O3	1.908 (13)
Fe3—O1 ⁱⁱ	1.829 (18)	Fe1—O3 ^{vi}	1.908 (13)
Fe3—O5	2.359 (14)	C1—O6	1.403 (19)
Fe3—O3 ^{iv}	2.127 (7)	C1—O2 ^v	1.288 (18)
Fe3—O3 ^v	2.127 (7)	C1—O5	1.411 (17)
Mg2—O4	1.84 (2)	C1—O3 ^x	1.28 (2)
Mg2—O2	1.813 (9)	C2—O4 ^{xi}	1.29 (3)
Mg2—O2 ⁱ	1.813 (9)	C2—O6	1.38 (2)
Mg2—O5	1.87 (2)	C2—O6 ⁱ	1.38 (2)
Mg2—O3	1.814 (9)	C2—O1 ^{xi}	1.34 (3)

O6—Mg3—O6 ⁱ	53.0 (3)	O5—Fe3—O3 ^{iv}	100.3 (3)
O6—Mg3—O2	91.1 (4)	O5—Fe3—O3 ^v	100.3 (3)
O6—Mg3—O2 ⁱⁱ	119.7 (3)	O3 ^{iv} —Fe3—O3 ^v	147.1 (5)
O6—Mg3—O2 ⁱⁱⁱ	159.8 (5)	O4—Mg2—O2	108.6 (6)
O6—Mg3—O2 ⁱ	121.8 (4)	O4—Mg2—O2 ⁱ	108.6 (6)
O6—Mg3—O1 ⁱⁱ	79.3 (6)	O4—Mg2—O5	166.6 (7)
O6—Mg3—O5	54.7 (5)	O4—Mg2—O3	85.1 (6)
O6—Mg3—O3 ^{iv}	112.4 (5)	O4—Mg2—O3 ⁱ	85.1 (6)
O6—Mg3—O3 ^v	61.7 (4)	O2—Mg2—O2 ⁱ	75.3 (4)
O6 ⁱ —Mg3—O2	121.8 (4)	O2—Mg2—O5	81.8 (6)
O6 ⁱ —Mg3—O2 ⁱⁱ	159.8 (5)	O2—Mg2—O3	97.4 (4)
O6 ⁱ —Mg3—O2 ⁱⁱⁱ	119.7 (3)	O2—Mg2—O3 ⁱ	165.8 (7)
O6 ⁱ —Mg3—O2 ⁱ	91.1 (4)	O2 ⁱ —Mg2—O5	81.8 (6)
O6 ⁱ —Mg3—O1 ⁱⁱ	79.3 (6)	O2 ⁱ —Mg2—O3	165.8 (7)
O6 ⁱ —Mg3—O5	54.7 (5)	O2 ⁱ —Mg2—O3 ⁱ	97.4 (4)
O6 ⁱ —Mg3—O3 ^{iv}	61.7 (4)	O5—Mg2—O3	85.1 (6)
O6 ⁱ —Mg3—O3 ^v	112.4 (5)	O5—Mg2—O3 ⁱ	85.1 (6)
O2—Mg3—O2 ⁱⁱ	74.2 (4)	O3—Mg2—O3 ⁱ	87.0 (4)
O2—Mg3—O2 ⁱⁱⁱ	107.0 (5)	O4—Mg1—O4 ^{vi}	69.1 (5)
O2—Mg3—O2 ⁱ	69.3 (4)	O4—Mg1—O6 ^v	73.9 (4)
O2—Mg3—O1 ⁱⁱ	144.2 (3)	O4—Mg1—O6 ^{vii}	139.3 (4)
O2—Mg3—O5	67.3 (5)	O4—Mg1—O1 ^{viii}	150.6 (7)
O2—Mg3—O3 ^{iv}	140.7 (5)	O4—Mg1—O1 ^{ix}	118.7 (6)
O2—Mg3—O3 ^v	71.5 (4)	O4—Mg1—O3	79.4 (6)
O2 ⁱⁱ —Mg3—O2 ⁱⁱⁱ	59.6 (3)	O4—Mg1—O3 ^{vi}	82.3 (6)
O2 ⁱⁱ —Mg3—O2 ⁱ	107.0 (5)	O4 ^{vi} —Mg1—O6 ^v	139.3 (4)
O2 ⁱⁱ —Mg3—O1 ⁱⁱ	80.8 (6)	O4 ^{vi} —Mg1—O6 ^{vii}	73.9 (4)
O2 ⁱⁱ —Mg3—O5	140.5 (4)	O4 ^{vi} —Mg1—O1 ^{viii}	118.7 (6)
O2 ⁱⁱ —Mg3—O3 ^{iv}	115.2 (4)	O4 ^{vi} —Mg1—O1 ^{ix}	150.6 (7)
O2 ⁱⁱ —Mg3—O3 ^v	58.1 (4)	O4 ^{vi} —Mg1—O3	82.3 (6)
O2 ⁱⁱⁱ —Mg3—O2 ⁱ	74.2 (4)	O4 ^{vi} —Mg1—O3 ^{vi}	79.4 (6)
O2 ⁱⁱⁱ —Mg3—O1 ⁱⁱ	80.8 (6)	O6 ^v —Mg1—O6 ^{vii}	146.1 (3)
O2 ⁱⁱⁱ —Mg3—O5	140.5 (4)	O6 ^v —Mg1—O1 ^{viii}	86.9 (5)
O2 ⁱⁱⁱ —Mg3—O3 ^{iv}	58.1 (4)	O6 ^v —Mg1—O1 ^{ix}	64.9 (5)
O2 ⁱⁱⁱ —Mg3—O3 ^v	115.2 (4)	O6 ^v —Mg1—O3	74.6 (5)
O2 ⁱ —Mg3—O1 ⁱⁱ	144.2 (3)	O6 ^v —Mg1—O3 ^{vi}	112.2 (5)
O2 ⁱ —Mg3—O5	67.3 (5)	O6 ^{vii} —Mg1—O1 ^{viii}	64.9 (5)
O2 ⁱ —Mg3—O3 ^{iv}	71.5 (4)	O6 ^{vii} —Mg1—O1 ^{ix}	86.9 (5)
O2 ⁱ —Mg3—O3 ^v	140.7 (5)	O6 ^{vii} —Mg1—O3	112.2 (5)
O1 ⁱⁱ —Mg3—O5	127.7 (8)	O6 ^{vii} —Mg1—O3 ^{vi}	74.6 (5)
O1 ⁱⁱ —Mg3—O3 ^{iv}	73.6 (3)	O1 ^{viii} —Mg1—O1 ^{ix}	69.7 (7)
O1 ⁱⁱ —Mg3—O3 ^v	73.6 (3)	O1 ^{viii} —Mg1—O3	74.1 (6)
O5—Mg3—O3 ^{iv}	100.3 (3)	O1 ^{viii} —Mg1—O3 ^{vi}	126.1 (6)
O5—Mg3—O3 ^v	100.3 (3)	O1 ^{ix} —Mg1—O3	126.1 (6)
O3 ^{iv} —Mg3—O3 ^v	147.1 (5)	O1 ^{ix} —Mg1—O3 ^{vi}	74.1 (6)
O6—Fe3—O6 ⁱ	53.0 (3)	O3—Mg1—O3 ^{vi}	157.8 (4)
O6—Fe3—O2	91.1 (4)	O4—Fe1—O4 ^{vi}	69.1 (5)
O6—Fe3—O2 ⁱⁱ	119.7 (3)	O4—Fe1—O6 ^v	73.9 (4)

O6—Fe3—O2 ⁱⁱⁱ	159.8 (5)	O4—Fe1—O6 ^{vii}	139.3 (4)
O6—Fe3—O2 ⁱ	121.8 (4)	O4—Fe1—O1 ^{viii}	150.6 (7)
O6—Fe3—O1 ⁱⁱ	79.3 (6)	O4—Fe1—O1 ^{ix}	118.7 (6)
O6—Fe3—O5	54.7 (5)	O4—Fe1—O3	79.4 (6)
O6—Fe3—O3 ^{iv}	112.4 (5)	O4—Fe1—O3 ^{vi}	82.3 (6)
O6—Fe3—O3 ^v	61.7 (4)	O4 ^{vi} —Fe1—O6 ^v	139.3 (4)
O6 ⁱ —Fe3—O2	121.8 (4)	O4 ^{vi} —Fe1—O6 ^{vii}	73.9 (4)
O6 ⁱ —Fe3—O2 ⁱⁱ	159.8 (5)	O4 ^{vi} —Fe1—O1 ^{viii}	118.7 (6)
O6 ⁱ —Fe3—O2 ⁱⁱⁱ	119.7 (3)	O4 ^{vi} —Fe1—O1 ^{ix}	150.6 (7)
O6 ⁱ —Fe3—O2 ⁱ	91.1 (4)	O4 ^{vi} —Fe1—O3	82.3 (6)
O6 ⁱ —Fe3—O1 ⁱⁱ	79.3 (6)	O4 ^{vi} —Fe1—O3 ^{vi}	79.4 (6)
O6 ⁱ —Fe3—O5	54.7 (5)	O6 ^v —Fe1—O6 ^{vii}	146.1 (3)
O6 ⁱ —Fe3—O3 ^{iv}	61.7 (4)	O6 ^v —Fe1—O1 ^{viii}	86.9 (5)
O6 ⁱ —Fe3—O3 ^v	112.4 (5)	O6 ^v —Fe1—O1 ^{ix}	64.9 (5)
O2—Fe3—O2 ⁱⁱ	74.2 (4)	O6 ^v —Fe1—O3	74.6 (5)
O2—Fe3—O2 ⁱⁱⁱ	107.0 (5)	O6 ^v —Fe1—O3 ^{vi}	112.2 (5)
O2—Fe3—O2 ⁱ	69.3 (4)	O6 ^{vii} —Fe1—O1 ^{viii}	64.9 (5)
O2—Fe3—O1 ⁱⁱ	144.2 (3)	O6 ^{vii} —Fe1—O1 ^{ix}	86.9 (5)
O2—Fe3—O5	67.3 (5)	O6 ^{vii} —Fe1—O3	112.2 (5)
O2—Fe3—O3 ^{iv}	140.7 (5)	O6 ^{vii} —Fe1—O3 ^{vi}	74.6 (5)
O2—Fe3—O3 ^v	71.5 (4)	O1 ^{viii} —Fe1—O1 ^{ix}	69.7 (7)
O2 ⁱⁱ —Fe3—O2 ⁱⁱⁱ	59.6 (3)	O1 ^{viii} —Fe1—O3	74.1 (6)
O2 ⁱⁱ —Fe3—O2 ⁱ	107.0 (5)	O1 ^{viii} —Fe1—O3 ^{vi}	126.1 (6)
O2 ⁱⁱ —Fe3—O1 ⁱⁱ	80.8 (6)	O1 ^{ix} —Fe1—O3	126.1 (6)
O2 ⁱⁱ —Fe3—O5	140.5 (4)	O1 ^{ix} —Fe1—O3 ^{vi}	74.1 (6)
O2 ⁱⁱ —Fe3—O3 ^{iv}	115.2 (4)	O3—Fe1—O3 ^{vi}	157.8 (4)
O2 ⁱⁱ —Fe3—O3 ^v	58.1 (4)	O6—C1—O2 ^v	107.8 (11)
O2 ⁱⁱⁱ —Fe3—O2 ⁱ	74.2 (4)	O6—C1—O5	103.5 (10)
O2 ⁱⁱⁱ —Fe3—O1 ⁱⁱ	80.8 (6)	O6—C1—O3 ^x	113.7 (17)
O2 ⁱⁱⁱ —Fe3—O5	140.5 (4)	O2 ^v —C1—O5	107.9 (17)
O2 ⁱⁱⁱ —Fe3—O3 ^{iv}	58.1 (4)	O2 ^v —C1—O3 ^x	110.6 (10)
O2 ⁱⁱⁱ —Fe3—O3 ^v	115.2 (4)	O5—C1—O3 ^x	112.8 (11)
O2 ⁱ —Fe3—O1 ⁱⁱ	144.2 (3)	O4 ^{xi} —C2—O6	114.7 (12)
O2 ⁱ —Fe3—O5	67.3 (5)	O4 ^{xi} —C2—O6 ⁱ	114.7 (12)
O2 ⁱ —Fe3—O3 ^{iv}	71.5 (4)	O4 ^{xi} —C2—O1 ^{xi}	110 (3)
O2 ⁱ —Fe3—O3 ^v	140.7 (5)	O6—C2—O6 ⁱ	105 (2)
O1 ⁱⁱ —Fe3—O5	127.7 (8)	O6—C2—O1 ^{xi}	105.7 (13)
O1 ⁱⁱ —Fe3—O3 ^{iv}	73.6 (3)	O6 ⁱ —C2—O1 ^{xi}	105.7 (13)
O1 ⁱⁱ —Fe3—O3 ^v	73.6 (3)		

Symmetry codes: (i) $x, -y, z$; (ii) $-x+1, y, -z+1$; (iii) $-x+1, -y, -z+1$; (iv) $-x+1/2, y-1/2, -z+1$; (v) $-x+1/2, -y+1/2, -z+1$; (vi) $-x, y, -z$; (vii) $x-1/2, -y+1/2, z-1$; (viii) $x-1/2, y+1/2, z$; (ix) $-x+1/2, y+1/2, -z$; (x) $-x, y, -z+1$; (xi) $x, y, z+1$.

Iron (II) Magnesium (II) carbonate (MgCO₃_98GPa)

Crystal data

Mg_{0.85}Fe_{0.15}CO₃

$M_r = 89$

Trigonal, $R\bar{3}c$

Hall symbol: $-R\ 3\ 2''c$

$a = 4.281 (7) \text{ \AA}$

$c = 12.12 (2) \text{ \AA}$

$V = 192.3 (5) \text{ \AA}^3$
 $Z = 6$
 $F(000) = 265$
 $D_x = 4.614 \text{ Mg m}^{-3}$
 Synchrotron radiation, $\lambda = 0.2952 \text{ \AA}$
 Cell parameters from 65 reflections

$\theta = 2.7\text{--}13.9^\circ$
 $\mu = 0.25 \text{ mm}^{-1}$
 $T = 293 \text{ K}$
 Irregular, colourless
 $0.01 \times 0.01 \times 0.01 \text{ mm}$

Data collection

13IDD @ APS (GSECARS)
 diffractometer
 Radiation source: synchrotron
 Synchrotron monochromator
 ω scans
 Absorption correction: multi-scan
 (CrysAlisPro; Rigaku OD, 2019)
 $T_{\min} = 0.95, T_{\max} = 1$

176 measured reflections
 60 independent reflections
 33 reflections with $I > 3\sigma(I)$
 $R_{\text{int}} = 0.053$
 $\theta_{\max} = 15.4^\circ, \theta_{\min} = 2.7^\circ$
 $h = -6 \rightarrow 6$
 $k = -7 \rightarrow 5$
 $l = -18 \rightarrow 18$

Refinement

Refinement on F
 Least-squares matrix: full
 $R[F^2 > 2\sigma(F^2)] = 0.100$
 $wR(F^2) = 0.084$
 $S = 2.89$
 60 reflections
 5 parameters

0 restraints
 1 constraint
 Weighting scheme based on measured s.u.'s $w =$
 $1/(\sigma^2(F) + 0.000144F^2)$
 $(\Delta/\sigma)_{\max} < 0.001$
 $\Delta\rho_{\max} = 0.66 \text{ e \AA}^{-3}$
 $\Delta\rho_{\min} = -0.50 \text{ e \AA}^{-3}$

Fractional atomic coordinates and isotropic or equivalent isotropic displacement parameters (\AA^2)

	x	y	z	$U_{\text{iso}}^*/U_{\text{eq}}$	Occ. (<1)
Mg1	0	0	0	0.0373 (13)*	0.85
Fe1	0	0	0	0.0373 (13)*	0.15
O1	0.2791 (17)	0	0.25	0.0382 (16)*	
C1	0	0	0.25	0.040 (3)*	

Geometric parameters ($\text{\AA}, ^\circ$)

Mg1—O1 ⁱ	1.855 (7)	Fe1—O1 ⁱⁱⁱ	1.855 (8)
Mg1—O1 ⁱⁱ	1.855 (5)	Fe1—O1 ^{iv}	1.855 (7)
Mg1—O1 ⁱⁱⁱ	1.855 (8)	Fe1—O1 ^v	1.855 (5)
Mg1—O1 ^{iv}	1.855 (7)	Fe1—O1 ^{vi}	1.855 (8)
Mg1—O1 ^v	1.855 (5)	C1—O1	1.195 (8)
Mg1—O1 ^{vi}	1.855 (8)	C1—O1 ^{vii}	1.195 (8)
Fe1—O1 ⁱ	1.855 (7)	C1—O1 ^{viii}	1.195 (8)
Fe1—O1 ⁱⁱ	1.855 (5)		
O1 ⁱ —Mg1—O1 ⁱⁱ	93.2 (2)	O1 ⁱ —Fe1—O1 ^{iv}	180
O1 ⁱ —Mg1—O1 ⁱⁱⁱ	93.2 (2)	O1 ⁱ —Fe1—O1 ^v	86.8 (2)
O1 ⁱ —Mg1—O1 ^{iv}	180	O1 ⁱ —Fe1—O1 ^{vi}	86.8 (2)
O1 ⁱ —Mg1—O1 ^v	86.8 (2)	O1 ⁱⁱ —Fe1—O1 ⁱⁱⁱ	93.2 (3)
O1 ⁱ —Mg1—O1 ^{vi}	86.8 (2)	O1 ⁱⁱ —Fe1—O1 ^{iv}	86.8 (2)
O1 ⁱⁱ —Mg1—O1 ⁱⁱⁱ	93.2 (3)	O1 ⁱⁱ —Fe1—O1 ^v	180
O1 ⁱⁱ —Mg1—O1 ^{iv}	86.8 (2)	O1 ⁱⁱ —Fe1—O1 ^{vi}	86.8 (3)

O1 ⁱⁱ —Mg1—O1 ^v	180	O1 ⁱⁱⁱ —Fe1—O1 ^{iv}	86.8 (2)
O1 ⁱⁱ —Mg1—O1 ^{vi}	86.8 (3)	O1 ⁱⁱⁱ —Fe1—O1 ^v	86.8 (3)
O1 ⁱⁱⁱ —Mg1—O1 ^{iv}	86.8 (2)	O1 ⁱⁱⁱ —Fe1—O1 ^{vi}	180
O1 ⁱⁱⁱ —Mg1—O1 ^v	86.8 (3)	O1 ^{iv} —Fe1—O1 ^v	93.2 (2)
O1 ⁱⁱⁱ —Mg1—O1 ^{vi}	180	O1 ^{iv} —Fe1—O1 ^{vi}	93.2 (2)
O1 ^{iv} —Mg1—O1 ^v	93.2 (2)	O1 ^v —Fe1—O1 ^{vi}	93.2 (3)
O1 ^{iv} —Mg1—O1 ^{vi}	93.2 (2)	O1—C1—O1 ^{vii}	120.00 (10)
O1 ^v —Mg1—O1 ^{vi}	93.2 (3)	O1—C1—O1 ^{viii}	120.0 (5)
O1 ⁱ —Fe1—O1 ⁱⁱ	93.2 (2)	O1 ^{vii} —C1—O1 ^{viii}	120.0 (5)
O1 ⁱ —Fe1—O1 ⁱⁱⁱ	93.2 (2)		

Symmetry codes: (i) $x-2/3, y-1/3, z-1/3$; (ii) $-y+1/3, x-y-1/3, z-1/3$; (iii) $-x+y+1/3, -x+2/3, z-1/3$; (iv) $-x+2/3, -y+1/3, -z+1/3$; (v) $y-1/3, -x+y+1/3, -z+1/3$; (vi) $x-y-1/3, x-2/3, -z+1/3$; (vii) $-y, x-y, z$; (viii) $-x+y, -x, z$.

Fractional atomic coordinates and isotropic displacement parameters of (Mg_{2.53}Fe_{0.47})C₃O₉ at 98 GPa.

Atom label	x	y	z	Site symmetry	U _{isco} ^[a]	Occupancy
Mg1	0	0.2457 (6)	0	4g	0.0117 (13)	0.917 (17)
Fe1	0	0.2457 (6)	0	4g	0.0117 (13)	0.083 (17)
Mg2	0.1712 (7)	0	0.3146 (12)	4i	0.0086 (11)	1
Mg3	0.4441 (6)	0	0.6503 (9)	4i	0.0177 (11)	0.61 (2)
Fe3	0.4441 (6)	0	0.6503 (9)	4i	0.0177 (11)	0.39 (2)
O1	0.4097 (18)	0	0.105 (3)	4i	0.021 (2)	1
O2	0.3442 (12)	0.1683 (9)	0.4218 (18)	8j	0.0157 (15)	1
O3	0.0062 (12)	0.1898 (9)	0.2702 (19)	8j	0.0159 (17)	1
O4	0.1395 (17)	0	0.044 (3)	4i	0.020 (2)	1
O5	0.1487 (16)	0	0.575 (3)	4i	0.016 (2)	1
O6	0.2736 (13)	0.1662 (9)	0.847 (2)	8j	0.0179 (17)	1
C1	0.1347 (19)	0.1774 (13)	0.683 (3)	8j	0.017 (2)	1
C2	0.265 (3)	0	0.964 (4)	4i	0.024 (3)	1

[a] All atomic displacement parameters were refined in the isotropic approximation

Fractional atomic coordinates and isotropic displacement parameters of (Mg_{0.85}Fe_{0.15})CO₃ at 98 GPa.

Atom label	x	y	z	Site symmetry	U _{isco} ^[a]	Occupancy
Mg1	0	0	0	6b	0.0373 (13)	0.85
Fe1	0	0	0	6b	0.0373 (13)	0.15
O1	0.2791 (17)	0	0.25	18e	0.0382 (16)	1
C1	0	0	0.25	6a	0.04 (3)	1

[a] All atomic displacement parameters were refined in the isotropic approximation